

Accepted Manuscript

Experimental study on CO₂ sorption capacity of the neat and porous silica supported ionic liquids and the effect of water content of flue gas

Mojtabai Mirzaei, Ali Reza Badiei, Babak Mokhtarani, Ali Sharifi

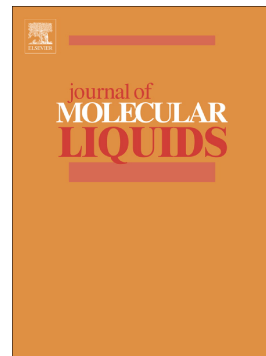
PII: S0167-7322(16)31538-0
DOI: doi: [10.1016/j.molliq.2017.02.104](https://doi.org/10.1016/j.molliq.2017.02.104)
Reference: MOLLIQ 7017

To appear in: *Journal of Molecular Liquids*

Received date: 13 June 2016
Revised date: 23 February 2017
Accepted date: 25 February 2017

Please cite this article as: Mojtabai Mirzaei, Ali Reza Badiei, Babak Mokhtarani, Ali Sharifi , Experimental study on CO₂ sorption capacity of the neat and porous silica supported ionic liquids and the effect of water content of flue gas. The address for the corresponding author was captured as affiliation for all authors. Please check if appropriate. Molliq(2017), doi: [10.1016/j.molliq.2017.02.104](https://doi.org/10.1016/j.molliq.2017.02.104)

This is a PDF file of an unedited manuscript that has been accepted for publication. As a service to our customers we are providing this early version of the manuscript. The manuscript will undergo copyediting, typesetting, and review of the resulting proof before it is published in its final form. Please note that during the production process errors may be discovered which could affect the content, and all legal disclaimers that apply to the journal pertain.



Experimental study on CO₂ sorption capacity of the neat and porous silica supported ionic liquids and the effect of water content of flue gas

Mojtabai Mirzaei [†], Ali Reza Badiei ^{*,†}, Babak Mokhtarani ^{*,‡} and Ali Sharifi [‡]

[†]School of Chemistry, College of Science, University of Tehran, Tehran, Iran

[‡] Chemistry and Chemical Engineering Research Center of Iran, P.O. Box 14335-186, Tehran, Iran.

Abstract:

In this research, absorption of CO₂ in different ionic liquids (ILs) is studied. Thus four ILs were synthesized containing 1-butyl-3-methylimidazolium as the cation and nitrate [NO₃]⁻, thiocyanate [SCN]⁻, dicyanamide [N(CN)₂]⁻ and hydrogen sulfate [HSO₄]⁻ as the anions, respectively. The resulting ILs were then immobilized into activated silica support in a 1/1 IL/SiO₂ weight ratio via the impregnation-vaporization method. CO₂ sorption behavior of both neat and silica supported ILs (ILs-SiO₂) were investigated at different temperatures and flow rates under atmospheric pressure, while their desorption process were carried out under 20 mmHg at 70°C. In both sorbents, the best results were obtained at 25°C with a flow rate of 12 mL/min, where [bmim][N(CN)₂] with 1.85 (wt%) or 0.42 mmol CO₂ per gram of sorbent and [bmim][HSO₄]-SiO₂ with 2.33 (wt%) or 0.53 mmol CO₂ per gram of sorbent showed the highest sorption capacities. The effect of water on CO₂ absorption capacity of the neat and silica supported ILs were also studied by transmission of CO₂ gas flue containing 400 ppm water. The results indicated that the mass gain was higher when wet CO₂ was passed through the sorbents, opposed to passing dry CO₂. Because of the existence of a weak coulombic interaction between the sorbents and CO₂, desorption occurs rapidly and a readily reuse of the sorbents is therefore provided.

Key words: Carbon dioxide, Sorption, Desorption, Supported ionic liquid, ILs-loaded silica

*Corresponding author *E-mail:* abadiei@ut.ac.ir Tel: +98-2161112614. Fax: +98-2161113301

*Corresponding author *E-mail:* mokhtarani@ccerci.ac.ir Tel.: +98 21 44787770; Fax: +98 21 44787781.

1. Introduction

With the beginning of the industrial revolution, the atmospheric CO₂ has faced an unexpected alarming growth and this event has been suggested to be a leading contributor to global climate change. In the wake of reductions in anthropogenic CO₂ emissions [1], and in large emission sources such as fossil-fuel-based power generation facilities, achieving an appropriate way to remove CO₂ as a predominant element in greenhouse phenomena is an important issue [2].

The traditional way for CO₂ absorption in natural gas sweetening is the use of aqueous alkanol amines that suffer from some intrinsic drawbacks like sorbent loss during recovery step, equipment corrosion together with high energy consumption in desorption process [3].

ILs that are generally composed of a large organic cation and organic or inorganic anions, have got good academically and industrially attention in recent decade. No flammability and corrosion, high thermal stability, negligible vapor pressure, a wide liquid range, electric conductivity following with their tunable physiochemical properties made them safer and more environmentally friendly than conventional organic absorbents [4]. In addition, selection diverse anions and cations, ILs with different chemical and physical properties could be produced.

ILs have been used as reaction media in separation [5], extraction processes [6], and furthermore, they seem suitable for being used as gas absorbent solvent [7].

First, Blanchard et al. [8], reported the solubility of CO₂ in 1-butyl-3-methylimidazolium hexafluorophosphate [bmim][PF₆]. The mole fraction of CO₂ in IL at 80 bar was 0.6. After Blanchard, a lot of research in absorption of CO₂ were reported [9-11]. For example, Anthony et al. [12], considered the CO₂ absorption of the two [bmim]-based ILs containing tetrafluoroborate [BF₄]⁻ and bis(trifluoromethane)sulfonimide [Tf₂N]⁻ as the anions and concluded that ILs with [Tf₂N]⁻ anion showed the better affinity for CO₂ absorption.

Aki et al. investigated the effect of the length of alkyl chains located on cation on CO₂ solubility and acclaimed that by increase of the alkyl chain length, CO₂ absorption capacity increases [13].

In another assessment the impact of the anions on CO₂ absorption capacity have been investigated and it was found that CO₂ solubility increased as follow [14], [C₇F₁₅CO₂]⁻ > [TF₂N]⁻ > [PF₆]⁻ > [DCA]⁻ > [BF₄]⁻ > [MeSO₄]⁻ > [SCN]⁻ > [NO₃]⁻

Mokhtarani et al. [15] have studied the solubility of CO₂ in three imidazolium-based ILs containing nitrate [NO₃]⁻ and thiocyanate [SCN]⁻ as the anions at 298.15 K to 333.15 K and pressure up to 45 bar. The studied ILs were 1-hexyl-3-methylimidazolium thiocyanate [hmim][SCN], 3-methyl-

1-octylimidazolium thiocyanate [omim][SCN] and 3-methyl-1-octylimidazolium nitrate [omim][NO₃]. The result showed that the [omim][NO₃] was more favorable for solubility of CO₂ than the both thiocyanate based ILs.

Kazarian et al. [16] observed that there are weak Lewis acid-base interactions between CO₂ molecules and the fluorinated anions in [bmim][BF₄] and [bmim][PF₆] and found that the interactions between CO₂ and anions have not played a decisive role in the solubility of CO₂ in ILs. They concluded that the CO₂ only occupies empty cavities created by the ions in the ILs structure.

Dissolution of CO₂ in ILs will be done physically or chemically. In conventional ILs, absorption can be carried out physically, therefore an effective absorption will be obtained in high pressure and low temperature [17]. Because of low gas absorption capacity in conventional ILs, researchers have looked for designing ILs containing effective groups in gas absorption process.

In this regard, Bates et al. [18] synthesized the first imidazolium based IL containing an amine group on the cation ring known as Task-Specific IL (TSIL) which improved the CO₂ absorption capacity compared to common ones. After 3 hours continuous passage of dry CO₂ through the TSIL at room temperature and 1 atmosphere of pressure, 7.4% weight gain was observed.

Phosphonium amino acid salts ILs with amino groups in anions [19], or in anions & cations [20], have showed better absorption capacity compared to corresponding imidazolium ILs [21].

Regarding the importance of acid gas elimination from continuous gas flue in industry, numerous reports were presented in this field. For example, Brennecke and co-workers [22], have investigated the ability of conventional IL 1-hexyl-3-methylimidazolium hexafluorophosphate [hmim][PF₆] when exposed to the continuous flue of CO₂ at 1 bar. Finally, there was only a 0.0881% mass gain in IL.

In another work, they showed that the CO₂ mole fraction in 1-butyl-3-methylimidazolium bis(trifluoromethane) sulfonimide [bmim][Tf₂N] at 1 bar was only 0.03, while the mole fraction of SO₂ in the same IL was 0.552 [12].

Elliott et al. [23], have reported the SO₂ solubility in some [bmim]-based ILs at 323 K and 1 bar pressure. Unexpected results demonstrated that, ILs with [Br]⁻ and [NO₃]⁻ as the anions had the highest SO₂ absorption capacity ([Br]⁻ ≈ [NO₃]⁻ > [Tf₂N]⁻ ≈ [BF₄]⁻ > [PF₆]⁻).

Park et al. [24] have used the imidazolium-based ILs containing ether functional group on the alkyl chain in CO₂ absorption process. They have seen that one mole of the ethereal group containing ILs were able to absorb 0.9 mol CO₂ at 30 °C.

The use of neat ILs in absorption process are not economically affordable because they are more expensive than conventional solvents [25]. In addition, the release of ILs in the environment, may

cause serious problems especially for the water sources. For example ILs with the fluorinated anions as [bmim][BF₄] and [bmim][PF₆] may be decomposed in the presence of water to give hydrofluoric and phosphoric acids. The toxicity of both ILs is the same as benzene [26].

so, researchers preferred to design new cost-effective sorbents containing a combination of small amount of ILs and large amounts of porous solid supports [25].

Several reviews on CO₂ capture by adsorption showed that adsorption with solid porous material as activated Carbon [27], Zeolites [28], Ordered mesoporous silica [29-31], has some benefit like low cost raw material, low heat capacity, fast kinetics, high CO₂ adsorption capacity and high CO₂ selectivity.

Future development in more operational adsorbents depend on designing of solid surfaces with new properties there with, immobilization of an IL on a solid support as a good solution, is a new approach to achieve this target [32].

When an IL immobilizes into solid supports, actually gives its specific properties to the solid substrate, which leads to a new sorbent with new efficiency. Because of large interfacial exchange area in solid supported ILs, mass transfer enhances and consequently, the gas absorption capacity improves [33].

Among solid supports, porous silica supports with regular pore structure attract a good attention and the presence of hydroxyl groups on the surface of mesoporous silica supports makes them an excellent candidate for the functionalization of the surface with the desired functional groups [34].

Wu and Zhu, et al. [35], considered SO₂ sorption/desorption behavior of the porous silica supported 1,1,3,3-tetramethylguanidinium lactate [tmgh][Lac] and introduced them as a good alternate for SO₂ removal. The IL was dispersed on silica particles via an incipient wetness technique. The SO₂ sorption was carried out at 1 bar at 20°C but desorption was done at 90°C under 80 mmHg vacuum.

Wu et al. [36] reported CO₂ adsorption capacity of N-(3-aminopropyl) aminoethyl tributylphosphonium amino acid ILs [Ts-P][amino acid] supported into silica particles and observed that in 1/1 weight ratio of TSIL and porous silica, IL containing Lysin as the anion with 1.55 (mmol CO₂)/(g TSIL) had the highest adsorption capacity, while adsorption capacity of the bare silica was 0.17 mmol CO₂/g SiO₂(0.75 wt%).

In other study, Zhu et al. [37] measured CO₂ capture capacity of grafted phosphonium IL [P₈₈₈₃][BF₄] on silica support. In this work, the IL was grafted on alkoxy-silyl modified silica and adsorption carried out at 40°C at 1 bar. The adsorption capacity of the bare and modified silica were higher than neat phosphonium-IL[P₈₈₈₃][BF₄]. Although the adsorption capacity of the bare silica was more than

IL-loaded silica, the CO₂/N₂ selectivity of IL-loaded silica and bare silica at 1 bar was too different, 8 and 3 respectively.

Jiang and co-workers [38], reported the solubility of SO₂ in some supported imidazolium-based ILs membranes at 298 K and 1 bar. They discerned that the [bmim][BF₄] had the highest absorption capacity. The mole fraction of adsorbed SO₂ was 0.57.

[bmim][BF₄] (0.57) > [bmim][NTf₂] ≈ [emim][BF₄] (0.551) > [bmim][PF₆] (0.536)

In this study, to reach more practical solid IL-containing CO₂ sorbent, it was tried to immobilize [bmim]⁺ type cation with the varieties of anions into the activated amorphous silica via impregnation-vaporization method [34] to do comparative evaluation between CO₂ absorption capacities of the neat and porous silica-supported ILs under continuous flue gas at 1 bar.

To this end, the CO₂ absorption capacities of the four neat and silica supported ILs at 25°C, 40°C and 50°C and ambient pressure was examined. The four ILs consisted of the same cation along with four different anions. The cation was 1-butyl-3-methylimidazolium [bmim]⁺ and the anions were nitrate [NO₃]⁻, thiocyanate [SCN]⁻, dicyanamide [N(CN)₂]⁻ and hydrogen sulfate [HSO₄]⁻.

2. Materials & methods

2.1. Materials

N-methylimidazole (98%, merck), 1-chlorobutane(98%), Silica- 60 (0.02-0.04 mm), hydrochloric acid (HCl, 37%), potassium thiocyanate (KSCN, 98%), sodium dicyanamide (NaN(CN)₂, 98%), sodium nitrate (NaNO₃, 98%,), silver nitrate (AgNO₃, 99.8%),phosphorus pentoxide (P₂O₅, 98%), sulfuric acid (98%), acetonitrile, ethyl acetate, ether, dichloromethane, acetone, and chloroform all were obtained from Merck Company. carbon dioxide (CO₂, ≥ 99.5%), methane (CH₄, ≥ 99.995%), nitrogen (N₂, ≥ 99.5%) were supplied by Pars Gas Company. The four used ILs and ILs-loaded silica support were synthesized in our Lab.

2.2. Synthesis and Immobilization of ILs into porous silica support

The [bmim][X]-SiO₂ were synthesized in a three-step process. Quaternized 1-butyl-3-methylimidazolium chloride [bmim][Cl] produced in the first step, underwent ionic exchange with the corresponding salt in the second stage to give desired ILs. Finally, the synthesized [bmim][X] immobilized into porous silica via impregnation-vaporization method.(Fig. SI-1).

2.2.1. Synthesis of [bmim][Cl]

1-butyl-3-methylimidazolium chloride [bmim][Cl] synthesized according to organic synthesis [39]. A mixture of 1-methylimidazole (1 eq) and 1-chlorobutane (1.3 eq) in dry acetonitrile was stirred at 75° C for 48 hours under nitrogen. The mixture was cooled to room temperature. The volatile material was removed under reduced pressure and the remaining light-yellow oil dissolved in appropriate acetonitrile and added dropwise to a flask containing dry ethyl acetate dry ethyl acetate containing flask to give [bmim][Cl] as a white crystal in approximately 82% yeild.

2.2.2. Synthesis of [bmim][NO₃], [bmim][SCN] and [bmim][N(CN)₂]

According to literature procedures [40], NaNO₃(1.1 eq), KSCN (1.2 eq) or NaN(CN)₂ (1.1 eq) was added to a solution of [Bmim][Cl] (1 eq) in dichloromethane and stirred for 24 h at room temperature.

The suspension was filtered to remove the produced NaCl and unreacted NaNO₃, KSCN and NaN(CN)₂ salts. The organic phase was repeatedly washed with small volume of water until no precipitation of AgCl occurred in the aqueous phase on addition of AgNO₃ solution. Then solvent was removed in vacuo and the synthesized IL was stirred with activated charcoal for 6h, removing the solvent gives [bmim][NO₃], [bmim][SCN] and [bmim][N(CN)₂] with 82%, 74% and 85% yields, respectively.

2.2.3. Synthesis of [bmim][HSO₄]

1-butyl-3-methylimidazolium hydrogen sulfate [bmim][HSO₄] was synthesized according to the reported procedures [41], by a dropwise addition of concentrated sulfuric acid (1 eq) to a cooled solution of 1-butyl-3-methylimidazolium chloride (1 eq) in anhydrous methylene chloride. The mixture was refluxed for 24h and the produced HCl was neutrilized by the aqueous solution of NaOH. Then, the solution was cooled to room temperature, consequently removing of solvent and then drying under vacuum at 75 °C for 3h gave yellow viscous liquid with 95% yeild.

2.2.4. Immobilization of [bmim][x] into porous silica support

Silica-60 powder was activated [42], by refluxing and stirring in hydrochloric acid (HCl, 6 M). After 24 h, the SiO₂ powder was filtered and washed with distilled water until to adjust the pH of the solution to 6-7. Then, the obtained wet solid was dried in 120°C for 6 h to give activated porous silica support. To avoid absorbing the air humidity the dried SiO₂ was kept in a desiccator.

In this work, the four ILs were immobilized into activated silica support via impregnation-vaporization method to produce ILs-loaded silica (ILs-SiO₂) [34]. To do this, suspension of 5 g IL

was mixed with 5 g of activated silica gel in ethanol and the mixture was stirred for 2 h. the solvent was removed in 50°C for 2h. After removing most of the solvent, wet powder was dried at 80°C under vacuum for 6h. The resulting [bmim][X]- SiO₂ sorbents were kept in a desiccator to avoid absorbing moisture before use (Fig. SI-1).

2.3. Characterization

The structures of the synthesized ILs were characterized by ¹H NMR (500 MHz) spectroscopy Bruker Advance 500 spectrometer in CD₃Cl and DMSO-d₆ at 25°C.

Density and viscosity of the neat ILs were measured with densitometer model DEM-5000-Anton paar and Anton Paar SVM 3000, respectively. The approximate water contents of the ILs before use were determined by Karl Fischer titration (KF-Coulometer 831). The water content of the CO₂ flue gas was measured by a vaisala humidity sensor (VAISALA HMP63)

A BELSORP-mini II Analyzer was used to measure the BET specific surface area and pore volume of the pure and IL- loaded silica using nitrogen at 77 K. First samples were degassed about 4 h at 10⁻³ bar and then the BET surface area was calculated from the nitrogen adsorption isotherm assuming area of nitrogen molecule to be 0.162 nm².

FTIR surface group chemistry analysis was performed using a Perkin-Elmer 400 spectrometer to identify the difference between blank and CO₂-rich sorbents.

Thermogravimetric analysis (TGA) of the neat and silica supported ILs were performed on a NETZSCH TG 209 F1 Iris instrument under nitrogen flue at a heating rate of 20 °C / min to 600 °C. The total chloride content was determined potentiometrically using a chloride ion selective electrode (ISE) in conjunction with a pH meter (Philips PW 9420) with an expanded millivolt scale.

3. Results and discussion

3.1. ¹H NMR, Density and viscosity, halide and water contents of synthesized ILs

The ¹H NMR data is presented at supplementary information (Fig. SI-2). The results confirm the structure of ILs synthesized. The water and chloride contents of the synthesized ILs were below 500 ppm except [bmim][HSO₄] whose chloride content was about 3000 ppm (Fig. SI-2). Density and viscosity of the neat ILs were summarized in Table 1[43-52].

3.2. Characteristics of the bare and ILs-loaded silica

The pore size distribution, specific surface area and porosity of the bare and ILs-loaded silica were identified by BET analysis (model:BELSORP-mini II). The activated amorphous silica used as support had a medium BET specific surface area of 369.8 m²/g, total pore volume of 0.79 cm³/g and average pore diameter of 8.53 nm. The pore size distribution (Fig. 1) showed that the majority of pores having diameters of less than 10 nm, indicating that mesopores (2 nm < pore diameter < 50 nm) have formed a majority of the pore volume. The N₂ adsorption-desorption isotherm (Fig. 2) of the activated silica was typical of a type IV material and the presence of Hysteresis type A confirmed that the mesoporous silica contains cylindrical pores.

As expected, The BET analysis identified that the ILs have immobilized into solid support and the specific surface area of the IL-loaded activated silica was significantly less than the bare activated silica. The effect of impregnation on the porosity of the silica support particles is shown in Table 2. It was obvious that the pore volume and surface area had a significant decrease. In the sorbent prepared at feed ratios of 0.25/1 and 0.5/1 of [bmim][NO₃]/SiO₂, the total pore volume (V_p) respectively decreased from 0.79 to 0.51 and 0.284 cm³/g and the specific surface area (A_p) reduced from 369.8 to 248.10 and 152.4 m²/g. While by impregnating of equal weight ratio of [bmim][NO₃] into porous silica, the total pore volume (V_p) will be decreased from 0.79 to 0.0004 cm³/g and the specific surface area (A_p) be changed from 369.8 to < 1 m²/g indicating that the micro & meso pores were completely filled with ILs and the surface area is truly the external surface of the activated silica support (Table 2). The pore size distribution of the bare and [bmim][NO₃]-loaded silica in various weight ratios have shown in Fig. 1.

The ILs-loaded silica sorbents were prepared by impregnation of certain weight ratio of IL into porous silica support, but as seen in Fig. 3, the actual amount of immobilized IL in sorbent was determined by thermogravimetric analysis (TGA).

As summarized in Table 2, according to TGA chromatogram (Fig. 3), the actual weight ratio of immobilized [bmim][NO₃] to silica support in [bmim][NO₃]-SiO₂ instead of 0.25, 0.50 and 1.00 were 0.247, 0.497 and 0.91 in order which represented the immobilization was incomplete. However, in [bmim][SCN]-SiO₂ the actual weight ratio of IL instead of 1.00 was 1.04.

In addition thermal stability of the neat ILs and ILs-loaded silica will be determined by TGA. Thermogravimetric analysis of the [bmim][NO₃], [bmim][SCN], [bmim][HSO₄], [bmim][NO₃]-SiO₂ and [bmim][SCN]-SiO₂ showed that they have a thermal decomposition temperature (T_d) above

250°C that approved their good thermal stability. It will be noted that by decrease of the IL portion in IL-loaded silica the thermal stability of the sorbent will be increased. For example thermal degradation of the neat [bmim][NO₃] begins from 250 °C while in [bmim][NO₃]-SiO₂ with weight ratios of 1/1 and 0.5/1 destruction begins from 280 °C and 350 °C, respectively. This approved that by immobilizing an IL into solid support, its thermal stability increases.

4. CO₂ sorption/desorption

The experimental apparatus was the same as described in literature [36], but for the neat ILs, instead of a U-tube, the sorption/desorption were carried out in a T-shaped glass reactor with input and output valves. (Fig. 4)

CO₂ was passed through P₂O₅ column in order to remove any existed humidity in the gas. The flow rate of CO₂ was controlled using a mass flow controller (Smart MFC Brooks, SLA5850), after stabilization of the flow rate at 12 ml/min, CO₂ enters into the T-shaped glass reactor and blows through the neat IL and goes out from the output valve for venting. The CO₂ sorption and desorption were determined gravimetrically. At preferred time, the glass reactor's valves were closed and the reactor was removed from water bath and weighted with an electronic balance (± 0.0001 g) to measure amount of adsorbed CO₂. The T-shaped glass then inserted to water bath again and this process has continued until reached to a constant weight.

In a typical method, 5 ml of the predried IL was transferred to a preweighed T-shaped glass. The IL in the T-shaped glass was further dried under vacuum at 70°C for 2 h in order to eliminate any impurity. Then, the T-shaped glass was filled with nitrogen and inserted into a preheated water bath (Open Bath\circulation Huber CC-K20) at desired temperature (25°C, 40°C or 50°C) for gas absorption.

For desorption stage, the T-shaped glass containing CO₂-rich IL was immersed into a preheated water bath and degassed under 20 mmHg pressure at 70°C. At the given time, it was filled with nitrogen, separated from the system and then weighted. This process has continued until no weight change observed in T-shaped glass reactor.

To evaluate the repeatability of the absorption/desorption cycle of ILs, some of tests were repeated 6 times. the experimental error of the repeated tests was $\pm 6\%$.

For ILs-loaded silica (ILs-SiO₂), the CO₂ sorption\desorption experiments were carried out in a U-tube [36]. The method was similar to that in neat ILs, however silica supported ILs ([bmim][X]-SiO₂) were used instead of the neat ILs.

4.1. CO₂ sorption/desorption of the neat ILs

The CO₂ sorption experiments were carried out at 1 atm of pressure at 25°C, 40°C and 50°C while, the desorption processes were performed under 20 mmHg at 70°C.

In order to obtain the best condition, the CO₂ sorption\desorption of the neat [bmim][NO₃] was studied in a T-shaped glass reactor at different temperature and gas flow rates of 12, 50 and 100 mL/min. Consequently, the best results were achieved at 25°C in a flow rate of 12 mL/min.(Fig. 5)

As seen in Fig. 2, the CO₂ sorption capacities of [bmim][NO₃] at 25°C, 40°C and 50°C were 1.42(wt%), 0.7 (wt%) and 0.42(wt%), respectively. In addition, the time of absorption, decreased from 1200 min at 25°C to 630 min at 40°C and 320 min at 50°C.

Gas absorption results of the four investigated neat ILs were shown in Fig. 6. Among them, [bmim][N(CN)₂] has the highest absorption capacity and the weight percent of absorbed CO₂(wt%) with a significant increase compared to [bmim][NO₃] raised to 1.85(wt%) at 25°C, 1.30 (wt%) at 40°C and 0.82(wt%) at 50°C.

As the results reveal, due to the use of the bubbling method, the absorption stage is time-consuming, and the temperature has a significant effect on the absorption capacity.

as summarized in Table 3, the CO₂ solubility order of the four tested ILs could be written as below:



there is approximately a linear dependency between the gas absorption capacity of the neat ILs and temperature i.e. an increase in temperature results in decreasing of gas absorption capacity. This dependency is shown in Fig. SI-3 of supporting information.

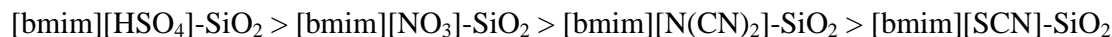
Unlike the absorption, the desorption was completed in less than 30 minutes. Such a fast desorption attributed to the absence of a specific functional group in ILs' structure to give strong link with CO₂. Fig. SI-4 shows the desorption process of studied ILs.

4.2. CO₂ sorption/desorption of the ILs-loaded silica

The CO₂ sorption\desorption of the silica supported ILs sorbents were studied in a U-tube glass reactor. To obtain the optimum conditions, the gas adsorption capacities of the [bmim][SCN]-SiO₂ with a flow rate of 12 ml/min at 25°C, 40°C and 50°C temperatures were measured and finally the best results were achieved in lower temperature. As shown in Fig. 7, the gas adsorption capacity decreases with an increase in temperature. CO₂ adsorption capacity of [bmim][SCN]-SiO₂ at 25°C

was 1.25 (wt%) but by increasing of temperature to 40°C and 50°C, the mass gain decreased to 0.66(wt%) and 0.37(wt%) respectively.

The CO₂ sorption of the four solid sorbents are shown in Fig. 8 and their results are listed in Table 3. According to the results, the CO₂ solubility order of the four tested SiO₂-ILs might be written as below:



Similar to the neat ILs, an approximately linear correlation between temperature and gas adsorption capacity of ILs-SiO₂ is shown in Fig. SI-5. According to this Figure, with increasing of temperature the gas absorption capacity of the solid sorbent are decreased.

As shown in Fig. SI-6, desorption stage of the ILs-SiO₂ sorbents almost like neat ILs were occurred in less than 30 minute.

At the end, it is noted that [bmim][N(CN)₂] with 1.85 (wt%) and [bmim][HSO₄]-SiO₂ with 2.33 (wt%) showed better sorption behaviour than the others.

4.3. CO₂ Sorption Mechanism

The silica used in this study had a CO₂ adsorption capacity of 0.82 (wt%). By impregnation of IL into porous silica support, silica surface was filled by IL and the existed silanol groups on silica surface have been engaged by ILs molecules. Thus, silica portion in gas absorption was reduced. Then, by the increase of IL weight percent in IL-loaded silica sorbent, CO₂ sorption capacity increases as well.

Due to lack of a strong link between CO₂ and the considered sorbents, adsorption could only be carried out physically [16], thus they have low absorption capacity; however, the major advantage of this weak linkage is the rapid desorption stage of the CO₂-rich sorbent, so the saturated liquid and solid sorbents can be easily recycled and are ready to use. FT-IR spectrum of the gas-treated sorbent has peak characteristic of dissolved CO₂ at 2340 cm⁻¹ [53].

5. Further Assessments for Practical Application

Effect of existed water in flue gas on CO₂ sorption

All used ILs in this study were able to adsorb the existed water in the flue gas, and since the CO₂ containing gas stream often contains certain amount of water, the effect of water on CO₂ absorption capacities of the neat and silica supported ILs were considered by transmission of CO₂ flue gas containing 400 ppm water. This amount of water was added to the gas cylinder by the gas supplier Company (Pars Gas Company).

Similar to the dry flue gas, by passing wet CO₂ through the sorbents, their CO₂ sorption capacities at 25°C, 40°C and 50°C in various flow rates was evaluated .

From a comparative view, after 1200 min passing the dry CO₂ through the neat [bmim][NO₃] at 25°C with a flow rate of 12 ml/min, the adsorbed CO₂ weight rise was 1.42 (wt%). However; at the same temperature and flow rate, by the pass of the CO₂ containing 400 ppm water, the observed mass gain was 3.10 (wt%) after 1800 min. (Fig. 9)

The results reveal that in case of wet gas, water together with CO₂ can be absorbed and finally reaches equilibrium at a specified time (Fig. 10). As seen in dry gas, temperature rise led to a decrease in gas adsorption capacity.

The full results of the wet gas absorption by neat ILs are presented in Table 3. According to the results, contrary to what was observed with dry gas, [bmim][NO₃] with 3.1(wt%) absorption had the highest absorption capacity among the four studied ILs (Fig. 11) while by passing the dry gas its absorption capacity was only 1.42 (wt%). As the studied ILs in this research are hydrophilic and the CO₂-containing about 400 ppm water, the ILs will absorb the water from flue gas and come into equilibrium with CO₂.

The wet gas capacity for studied ILs follows from this order: [bmim][NO₃] > [bmim][HSO₄] > [bmim][N(CN)₂] > [bmim][SCN],

however for dry gas the following order was observed.

[bmim][N(CN)₂] > [bmim][NO₃] > [bmim][HSO₄] > [bmim][SCN]

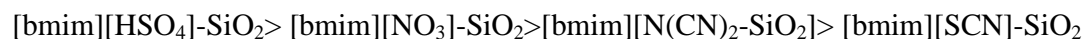
The outcomes clarified that there are a linear dependency between mass increase of neat ILs by wet CO₂ passage and temperature where an increase in temperature resulted a decrease in gas absorption capacity. (Fig. SI-7)

The impact of the existed water in flue gas on gas adsorption capacity of the ILs-loaded silica was also investigated. The results are reported in Table 3. As the results are shown, the weight will be additionally increased by passing the wet gas rather than the dry gas.

Wet gas

[bmim][NO₃]-SiO₂ > [bmim][N(CN)₂]-SiO₂ > [bmim][SCN]-SiO₂ > [bmim][HSO₄]-SiO₂

Dry gas



Among the four solid sorbents, $[\text{bmim}][\text{NO}_3]\text{-SiO}_2$ had the highest absorption capacity by transmission of wet CO_2 . (Fig. SI-8)

Effect of IL loading on CO_2 sorption

The effect of weight percent of $[\text{bmim}][\text{NO}_3]$ in $[\text{bmim}][\text{NO}_3]\text{-SiO}_2$ on adsorption capacity was determined. It was founded that an increase to the $[\text{bmim}][\text{NO}_3]/\text{SiO}_2$ ratio ($\phi_{\text{w,IL}}$ (g IL/g sorb)) led to the increase of the CO_2 sorption capacity but much time needs to reach equilibrium (Table 4). The $\phi_{\text{w,IL}}=0$ in Table 5 relates to the bare silica support.

By charting CO_2 sorption capacity of $[\text{bmim}][\text{NO}_3]\text{-SiO}_2$ in terms of weight fraction of $[\text{bmim}][\text{NO}_3]$ in the solid sorbent ($\phi_{\text{w,IL}}$ (g IL/g sorb)), an approximately linear dependency is observed where CO_2 (wt%) increases linearly by the increase of $\phi_{\text{w,IL}}$ (Fig. SI-9).

Effect of gas flow rate on CO_2 sorption

The effect of feed gas flow rate on gas absorption capacity of the neat and silica supported ILs were considered. As shown in Table 5, in similar condition, by the increase of the gas flow rate, the CO_2 sorption capacity reduces [54]. In higher gas flow rate the CO_2 residence time on the solid or liquid sorbent will be shortened that causes an uneffective interaction between CO_2 molecules and sorbents. For example in $[\text{Bmim}][\text{N}(\text{CN})_2]$ by the pass of the wet CO_2 with a flow rate of 12 ml/min, the absorption capacities at 25°C and 40°C were 2.73(wt%) and 1.82(wt%), respectively, but with a rise in CO_2 flow rate to 50 ml/min the sorption capacities reduced to 1.71(wt%) at 25°C and 0.8(wt%) at 40°C.

Comparing the CH_4 and CO_2 sorption capacity of the bare and IL-loaded silica

The bare and ILs-loaded silica can be used in natural gas sweetening. However, in order to investigate which one is better, it is necessary to measure the absorption capacity for CH₄. The CH₄ absorption capacity of the bare silica and [bmim][NO₃]-loaded silica which was prepared in 1/1 weight ratio of [bmim][NO₃] and silica were measured at 25 °C and 1 bar pressure. The results are summarized in Table 6. As the Table is shown by passing dry pure CH₄ in a flow rate of 12 ml/min through [bmim][NO₃]-SiO₂ about 0.162 (wt%) mass gain was observed, while the obtained mass rising from the dry CO₂ passage was 1.55 (wt%); i.e. the [bmim][NO₃]-loaded silica is able to absorb CO₂ about 9.68 times more than CH₄. In contrast, by passing dry CH₄ through the bare activated silica, the weight gain was 0.51(wt %) which has no big difference with CO₂ absorption capacity of bare silica (0.82 wt %) at the same condition. It was founded by decreasing the [bmim][NO₃] weight fraction from 0.50 to 0.334, the CH₄ absorption capacity raised from 0.16 (wt%) to 0.22 (wt%) and consequently the selectivity decreased from 9.68 to 6.36. It is true to say that ILs plays a key role in CO₂ absorption from natural gas stream.

Conclusion

In this study, four [bmim][X]-based ILs were synthesized and immobilized into porous silica supports in 1/1 weight ratio of SiO₂ and ILs. They showed good thermal stability up to 300°C. After characterizing the sorbents, their CO₂ adsorption\desorption were considered in diverse temperatures and flow rates. The best results for CO₂ adsorption by neat and silica supported ILs were obtained at 25°C with a flow rate of 12 mL/min, where [bmim][N(CN)₂] and [bmim][HSO₄]-SiO₂ with 1.85 (wt%) and 2.33 (wt%), respectively had the highest absorption capacities.

Despite the decline of ILs contribution in [bmim][X]-SiO₂, their CO₂ absorption capacities were more than those of neat ILs. For instance, by transmission of dry CO₂ with a flow rate of 12 ml/min through neat [bmim][NO₃], it indicated 1.42 (wt%) mass gain, while [bmim][NO₃]-loaded silica in 1/1 weight ratio of [bmim][NO₃] and SiO₂, the CO₂ absorption capacity raised to 1.55(wt%) that it is related to the synergic effect of the [bmim][NO₃] and porous silica support.

Under the same conditions, the gas flow rate significantly influenced the CO₂ absorption capacity of sorbents, low flow rates led to the higher absorption capacity.

The effect of the existed water in flue gas on the absorption capacities of the sorbents was also examined. It was discerned that the water together with CO₂ would be absorbed by neat and silica supported ILs. The results revealed that by transition of CO₂ containig 400 ppm water through the

sorbents, [bmim][NO₃] and [bmim][NO₃]-SiO₂ with 2.33(wt%) and 3.10 (wt%) had the highest absorption capacities.

According to the achieved outcomes, an increase in the IL/SiO₂ weight ratio has led to the CO₂ sorption capacity increase.

Meanwhile the CH₄ adsorption capacities of the bare and [bmim][NO₃]-loaded silica prepared in 1/1 weight ratio of [bmim][NO₃] and silica were measured. The result showed the high ability of [bmim][NO₃]-SiO₂ in absorbing CO₂ about 9.6 times compared to CH₄, while the bare silica absorbed CO₂ twice as much as CH₄. So, the ILs-loaded silica have better efficiency in CO₂ separation from natural gas. Due to the lack of appropriate functional groups on the neat and silica supported ILs, they could be easily recycled and reused in less than 30 minutes.

References

- [1] International Energy Agency, Tracking industrial energy efficiency and CO₂ emissions, OECD/IEA, Paris, 2007.
- [2] D. Bonenfant, M. Mimeault, R. Hausler, Determination of the structural features of distinct amines important for the absorption of CO₂ and regeneration in aqueous solution, *Ind. Eng. Chem. Res.* 42(2003) 3179-3184.
- [3] F. Zhang, C. G. Fang, Y. T. Wu, Y. T. Wang, A. M. Li, Z. B. Zhang, Absorption of CO₂ in the aqueous solutions of functionalized ionic liquids and MDEA, *Chem. Eng. J.* 160 (2010) 691-697.
- [4] M. Hasib-ur-Rahman, M. Sijaj, F. Larachi, Ionic liquids for CO₂ capture—development and progress, *Chem. Eng. Process.* 49(2010)313-322.
- [5] J. Palgunadi, H. S. Kim, J. M. Lee, S. Jung, Ionic liquids for ethyne and ethene separation: material selection and solubility investigation, *Chem. Eng. Process.* 49(2010) 192-198.
- [6] G. W. Meindersma, A. B. de Haan, Conceptual process design for aromatic/aliphatic separation with ionic liquids, *Proceedings of European Congress of Chemical Engineering (ECCE-6) Copenhagen*, 16-20 (Sep 2007).
- [7] L. M. Galan Sanchez, G. W. Meindersma, A. B. de Haan, Solvent properties of functionalized ionic liquids for CO₂ absorption, *Trans IChemE, Part A, Chem. Eng. Res. Des.* 85(A1) 200731-39.

- [8] L. A. Blanchard, D. Hancu, E. J. Beckman, J. F. Brennecke, Green processing using ionic liquids and CO₂, *Nature* 399 1999 28-29.
- [9] P. Scovazzo, D. Camper, J. Kieft, J. Poshusta, C. Koval, R. D. Noble, Regular solution theory and CO₂ gas solubility in room temperature ionic liquids, *Ind. Eng. Chem. Res.* 43(2004) 6855-6860.
- [10] A. Maiti, Theoretical screening of ionic liquid solvents for carbon capture, *ChemSusChem*. 2 (2009) 628-631.
- [11] T. K. Carlisle, J. E. Bara, C. J. Gabriel, R. D. Noble, D. L. Gin, Interpretation of CO₂ solubility and selectivity in nitrile-functionalized room-temperature ionic liquids using a group contribution approach, *Ind. Eng. Chem. Res.* 47(2008) 7005-7012.
- [12] J. L. Anthony, J. L. Anderson, E. J. Maginn, J. F. Brennecke, Anion effects on gas solubility in ionic liquid, *J. Phys. Chem. B* 109(2005) 6366-6374.
- [13] S. N. V. K. Aki, B. R. Mellein, E. M. Saurer, J. F. Brennecke, High-pressure phase behavior of carbon dioxide with imidazolium-based ionic liquids. *J. Phys. Chem. B* 108 (2004) 20355-20365.
- [14] M. Ramdin, T. W. de Loos, T. J. H. Vlucht, State-of-the-art of CO₂ capture with ionic liquids, *Ind. Eng. Chem. Res.* 51 (2012) 8149-8177.
- [15] B. Mokhtarani, A. Negar Khatun, M. Mafi, A. Sharifi, M. Mirzaei, Experimental study on the solubility of carbon dioxide in nitrate and thiocyanate-based ionic liquids, *J. Chem. Eng. Data* 61 (2016) 1262-1269.
- [16] S. G. Kazarian, B. J. Briscoe, T. Welton, Combining ionic liquids and supercritical fluids: ATR-IR study of CO₂ dissolved in two ionic liquids at high pressures, *Chem. Commun.* (2000) 2047-2048.
- [17] J. Huang, T. R  ther, Why are ionic liquids attractive for CO₂ absorption? An overview, *Aust. J. Chem.* 62(2009) 298-308.
- [18] E. D. Bates, R. D. Mayton, I. Ntai, J. H. Davis, CO₂ capture by a task-specific ionic liquid, *J. Am. Chem. Soc.* 124(2002) 926-927.

- [19] J. M. Zhang, S. J. Zhang, K. Dong, Y. Q. Zhang, Y. Q. Shen, X. M. Lu, Supported absorption of CO₂ by tetrabutylphosphonium amino acid ionic liquids, *Chem. Eur. J.* 12 (2006) 4021-4026.
- [20] Y. Q. Zhang, S. J. Zhang, X. M. Lu, Q. Zhou, W. Fan, X. P. Zhang, Dual amino-functionalized phosphonium ionic liquids for CO₂ capture, *Chem. Eur. J.* 15(2009) 3003-3011.
- [21] K. Fukumoto, M. Yoshizawa, H. Ohno, Room temperature ionic liquids from 20 natural amino acids, *J. Am. Chem. Soc.* 127 (2005) 2398-2399.
- [22] L. A. Blanchard, Z. Gu, J. F. Brennecke, High-pressure phase behavior of ionic liquid/CO₂ systems, *J. Phys. Chem. B* 105 (2001) 2437-2444.
- [23] A. F. Ghobadi, V. Taghikhani, R. Elliott, Investigation on the solubility of SO₂ and CO₂ in imidazolium-based ionic liquids using NPT Monte Carlo Simulation, *J. Phys. Chem. B* 115 (2011) 13599-13607.
- [24] P. Sharma, S. D. Park, K. T. Park, S. K. Jeong, S. C. Nam, H. Baek, Equimolar carbon dioxide absorption by ether functionalized imidazolium ionic liquids, *Bull. Korean Chem. Soc.* 33 (2012) 2325-2332.
- [25] M. Althuluth, J. P. Overbeek, H. J. V. Wees, L. F. Zubeir, W. G. Haije, A. Berrouk, C. J. Peters, M. C. Kroon, Natural gas purification using supported ionic liquid membrane, *J. Membr. Sci.* 484(2015) 80-86.
- [26] S. Keskin, D. Kayrak-Talay, U. Akman, O. Hortaçsu, A review of ionic liquids toward supercritical fluid applications, *J. Supercrit. Fluids* 43 (2007) 150-180.
- [27] M.G. Plaza, S. García, F. Rubiera, J. J. Pis, C. Pevida, Post-combustion CO₂ capture with a commercial activated carbon : Comparison of different regeneration strategies, *Chem. Eng. J.* 163(2010) 41-47.
- [28] Q. Wang, J. Luo, Z. Zhong, A. Borgna, CO₂ capture by solid adsorbents and their applications: current status and new trends, *Energy Environ. Sci.* 4(2011b) 42-55.
- [29] X. Liu, J. Li, L. Zhou, D. Huang, Y. Zhou, Adsorption of CO₂, CH₄ and N₂ on ordered mesoporous silica molecular sieve, *Chem. Phys. Lett.* 415(2005) 198-201.

- [30]Y. Sun, X. W. Liu, W. Su, Y. Zhou, L. Zhou, Studies on ordered mesoporous materials for potential environmental and clean energy applications, *Appl. Surf. Sci.* 253(2007) 5650-5655.
- [31]T. L. Chew, A. L. Ahmad, S. Bhatia, Ordered mesoporous silica (OMS) as an adsorbent and membrane for separation of carbon dioxide, *Adv. Colloid Interface Sci.* 153(2010)43-57.
- [32]F. Kohler, D. Roth, E. Kuhlmann, P. Wasserscheid, M. Haumann, Continuous gas-phase desulfurisation using supported ionic liquid phase (SILP) materials, *Green Chem.* 12 (2010) 979-984.
- [33]C. V. Doorslaer, J. Wahlen, P. Mertens, K. Binnemans, D. D. Vos, Immobilization of molecular catalysts in supported ionic liquid phases, *Dalton Trans.* 39(2010) 8377-8390.
- [34]M. H. Valkenberg, C. de Castro, W. F. Holderich, Immobilisation of ionic liquids on solid supports, *Green Chem.* 4 (2002)88-93.
- [35]Z. Zhang, L. Wu, J. Dong, B. G. Li, S. Zhu, Preparation and SO₂ sorption/desorption behavior of an ionic liquid supported on porous silica particles, *Ind. Eng. Chem. Res.* 48 (2009) 2142-2148.
- [36]J. Ren, L. Wu, B. G. Li, Preparation and CO₂ sorption/desorption of N-(3-aminopropyl) aminoethyl tributylphosphonium amino acid salt ionic liquids supported into porous silica particles, *Ind. Eng. Chem. Res.* 51(2012) 7901-7909.
- [37]J. Zhu, F. Xin, J. Huang, X. Dong, H. Liu, Adsorption and diffusivity of CO₂ in phosphonium ionic liquid modified silica, *Chem. Eng. J.* 246(2014)79-87.
- [38]Y. Y. Jiang, Z. Zhou, Z. Jiao, L. Li, Y. T. Wu, Z. B. Zhang, SO₂ gas separation using supported ionic liquid membranes, *J. Phys. Chem. B* 111 (2007) 5058-5061.
- [39]J. Dupont, C. S. Consorti, P. A. Z. Suarez, R. F. de Sousa, Preparation of 1-butyl-3-methyl imidazolium-based room temperature ionic liquids, *Org. Synth.* 79(2002) 236-243.
- [40]L. Cammarata, S. G. Kazarian, P. A. Salter, T. Welton, Molecular states of water in room temperature ionic liquid, *Phys. Chem. Chem. Phys.* 3 (2001) 5192-5200.
- [41]H. Tajik, K. Niknam, F. Parsa, Using acidic ionic liquid 1-butyl-3-methylimidazolium hydrogen sulfate in selective nitration of phenols under mild conditions, *J. Iran. Chem. Soc.* 6 (2009)159-164.

- [42]M. E. Mahmoud, H. M. Al-Bishri, Supported hydrophobic ionic liquid on nano-silica for adsorption of lead, *Chem. Eng. J.* 166 (2011) 157-167.
- [43]B. Mokhtarani, A. Sharifi, H. R. Mortaheb, M. Mirzaei, M. Mafi, F. Sadeghian, Density and viscosity of 1-butyl-3-methylimidazolium nitrate with ethanol, 1-propanol, or 1-butanol at several temperatures, *J. Chem. Thermodyn.* 41 (2009) 1432-1438.
- [44]K. R. Seddon, A. Stark, M.-J. Torres, Viscosity and density of 1-alkyl-3-methylimidazolium ionic liquids, *ACS Symp. Ser.* 819(2002) 34-49.
- [45]M. Larriba, P. Navarro, J. Garcia, F. Rodriguez, Selective extraction of toluene from n-heptane using [emim][SCN] and [bmim][SCN] ionic liquids as solvents, *J. Chem. Thermodyn.* 79 (2014) 266-271.
- [46]C. A. Nieto de Castro, E. Langa, A. L. Morais, M. L. S. M. Lopes, M. J. V. Lourenco, F. J. V. Santos, M. S. Santos, J. N. C. Lopes, H. M. Veiga, M. Macatrao, J. M. S. S. Esperanca, C. S. Marques, L. P. N. Rebelo, C. A. M. Afonso, Studies on the density, heat capacity, surface tension and infinite dilution diffusion with the ionic liquids [C4mim][NTf2], [C4mim][dca], [C2mim][EtOSO3] and [Aliquat][dca], *Fluid Phase Equilib.* 294 (2010)157-179.
- [47]M. Engelmann, H. Schmidt, J. Safarov, J. Nocke, E. Hassel, Thermal properties of 1-butyl-3-methylimidazolium dicyanamide at high pressures and temperatures, *Acta Chim. Slovaca*, 5(2012)86-94.
- [48]P. J. Carvalho, T. Regueira, L. M. N. B. F. Santos, J. Fernandez, J. A. P. Coutinho, Effect of water on the viscosities and densities of 1-butyl-3-methylimidazolium dicyanamide and 1-butyl-3-methylimidazolium tricyanomethane at atmospheric pressure, *J. Chem. Eng. Data* 55 (2010) 645-652.
- [49]R. G. Seoane, S. Corderi, E. Gomez, N. Calvar, E. J. Gonzalez, E. A. Macedo, A. Dominguez, Temperature dependence and structural influence on the thermophysical properties of eleven commercial ionic liquids, *Ind. Eng. Chem. Res.* 51 (2012)2492-2504.
- [50] X. Wang, H. Fan, T. Cui, Thermodynamic property of ionic liquid [Bmim][HSO₄], *Acta Sci. Nat. Univ. Sunyatseni* 51 (2012) 79-82.

- [51] B. Yoo, A. Afzal, J. M. Prausnitz, Henry's constants and activity coefficients of some organic solutes in 1-butyl,3-methylimidazolium hydrogen sulfate and in 1-methyl,3-trimethylsilylmethylimidazolium chloride, *J. Chem. Thermodyn.* 57 (2013) 178-181.
- [52] M. S. AlTuwaim, K. H. A. E. Alkhaldi, A. S. Al-Jimaz, A. A. Mohammad, Temperature Dependence of Physicochemical Properties of Imidazolium-, Pyrrolidinium-, and Phosphonium-Based Ionic Liquids, *J. Chem. Eng. Data* 59 (2014) 1955-1963.
- [53] J-M. Andanson, F. Jutz, A. Baiker, Purification of ionic liquids by supercritical CO₂ monitored by infrared spectroscopy, *J. of Supercritical Fluids* 55 (2010) 395-400
- [54] G. Severa, K. Bethune, R. Rocheleau, S. Higgins, SO₂ sorption by activated carbon supported ionic liquids under simulated atmospheric conditions *Chemical Engineering Journal* 265 (2015) 249-258.

Table 1. Density and viscosity of the synthesized ILs at different temperatures.

Ionic Liquid	Density (kg/m ³)			Viscosity (mPa.s)		
	25°C	40°C	50°C	25°C	40°C	50°C
[bmim][NO ₃]	1154.77 ^a	1145.47 ^a	1138.00 ^a	0.2107 ^a	0.09302 ^a	0.05495 ^a
	1156.5 ⁴³	1147 ⁴³	1140.7 ⁴³	0.1653 ⁴³	0.0828 ⁴³	0.0446 ⁴³
		1144 ⁴⁴	1137 ⁴⁴		0.085 ⁴⁴	0.0541 ⁴⁴
[bmim][SCN]	1073.02 ^a	1063.7 ^a	1057.7 ^a	0.0622 ^a	0.03224 ^a	0.02281 ^a
	1071.04 ⁴⁵	1062.21 ⁴⁵	1056.39 ⁴⁵	0.0598 ⁴⁵	0.0322 ⁴⁵	0.02297 ⁴⁵
[bmim][N(CN) ₂]	1059.76 ^a	1050.29 ^a	1044.05 ^a	0.03005 ^a	0.01788 ^a	0.01338 ^a
		1051 ⁴⁶	1044.8 ⁴⁶	0.0299 ⁴⁷	0.0177 ⁴⁷	0.0133 ⁴⁷
	1063.1 ⁴⁸	1053.7 ⁴⁸	1047.5 ⁴⁸	0.0318 ⁴⁸	0.0185 ⁴⁸	0.01378 ⁴⁸
	1060.46 ⁴⁹	1050.97 ⁴⁹	1044.72 ⁴⁹	0.03005 ⁴⁹	0.01777 ⁴⁹	0.0133 ⁴⁹
[bmim]HSO ₄	1282.2 ^a	1270.3 ^a	1258.5 ^a	0.355 ^a	0.166 ^a	0.114 ^a
	1220.1 ⁵⁰	1200.6 ⁵⁰	1187.3 ⁵⁰			
		1269 ⁵¹	1263.4 ⁵¹			
	1224 ⁵²	1214 ⁵²	1208 ⁵²	0.439 ⁵²	0.184 ⁵²	0.1124 ⁵²

^athis work**Table 2.** Pore characteristics^a of the bare SiO₂, [bmim][NO₃]- SiO₂ and [bmim][SCN]- SiO₂ sorbents.

Sample	IL/SiO ₂ ^b	IL/SiO ₂ ^c	V _p (cm ³ /g)	A _p (cm ² /g)	r _p (nm)
SiO ₂	0/1	0	0.7891	369.8	8.53
[bmim][NO ₃]- SiO ₂	0.25/1	0.247	0.51	248.10	7.93
[bmim][NO ₃]- SiO ₂	0.5/1	0.497	0.2843	152.4	7.46
[bmim][NO ₃]- SiO ₂	1/1	0.91	0.0004	< 1	< 1
[bmim][SCN]- SiO ₂	1/1	1.04	0.0031	< 2	< 1

^aV_p, A_p and r_p are total intrusion volume, specific surface area and average pore radius, respectively. ^bIL/SiO₂ ratio in feed, ^cIL/SiO₂ in solid sorbent.

Table 3: CO₂ sorption capacity of the neat ILs and ILs-loaded silica by the pass of the wet and dry CO₂ with a flow rate of 12 mL/min.

Sorbent	CO ₂ (w%)					
	25 °C		40°C		50°C	
	Dry	Wet	Dry	Wet	Dry	Wet
[bmim][NO ₃]- SiO ₂	1.55	2.33	0.79	1.47	0.53	1.20
[bmim][NO ₃]	1.42	3.10	0.70	1.78	0.43	1.31
[bmim][SCN]- SiO ₂	1.25	1.95	0.66	1.22	0.37	0.85
[bmim][SCN]	1.10	1.40	0.69	1.24	0.55	0.68
[bmim][N(CN) ₂]- SiO ₂	1.32	2.07	0.86	0.87	0.84	
[bmim][N(CN) ₂]	1.85	2.73	1.31	1.82	0.82	1.25
[bmim][HSO ₄]- SiO ₂	2.33	1.65	1.41	1.10	0.94	0.88
[bmim][HSO ₄]	1.34	3.00	1.13	2.10	0.78	1.42

Table 4. The effect of the [bmim][NO₃] weight fraction on CO₂ absorption capacity of SiO₂-[bmim][NO₃].

[bmim][NO ₃]/SiO ₂	0	1/3	1/2	1/1
φ _{w,IL} (g IL/g sorb)	0	0.25	0.334	0.5
CO ₂ (w%)	0.82	1.1	1.4	1.55

Table 5. The effect of wet CO₂ flow rate on absorption capacity of [bmim][N(CN)₂] and [bmim][NO₃]-SiO₂.

sorbent	CO ₂ (wt%)								
	12 mL/min			50 mL/min			100 mL/min		
	25 °C	40 °C	50 °C	25 °C	40 °C	50 °C	25 °C	40 °C	50 °C
[bmim][N(CN) ₂]	2.73	1.82	1.25	1.71	0.80				
[bmim][NO ₃]-SiO ₂	2.33	1.47	0.97	1.93	0.84	0.55	0.60		

Table 6: CH₄ sorption capacity of the bare and [bmim][NO₃]-loaded silica by the pass of the dry CH₄ with a flow rate of 12 mL/min.

Sorbent	g IL/ gIL-SiO ₂	CO ₂ (wt %)	CH ₄ (wt %)	Selectivity
SiO ₂	0	0.82	0.51	1.60
[bmim][NO ₃]-SiO ₂	0.25	1.10	-	-
[bmim][NO ₃]-SiO ₂	0.334	1.40	0.22	6.36
[bmim][NO ₃]-SiO ₂	0.50	1.55	0.16	9.68

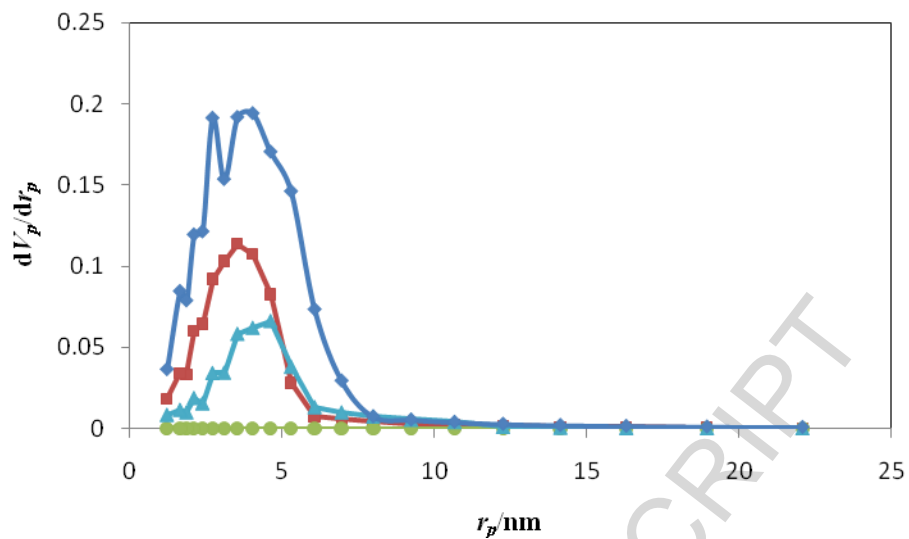


Figure 1. Pore size distribution of the activated bare silica (\diamond), [bmim][NO₃]-SiO₂ at weight ratios of 1/3 (\blacksquare), 1/2 (\blacktriangle) and 1/1 (\bullet).

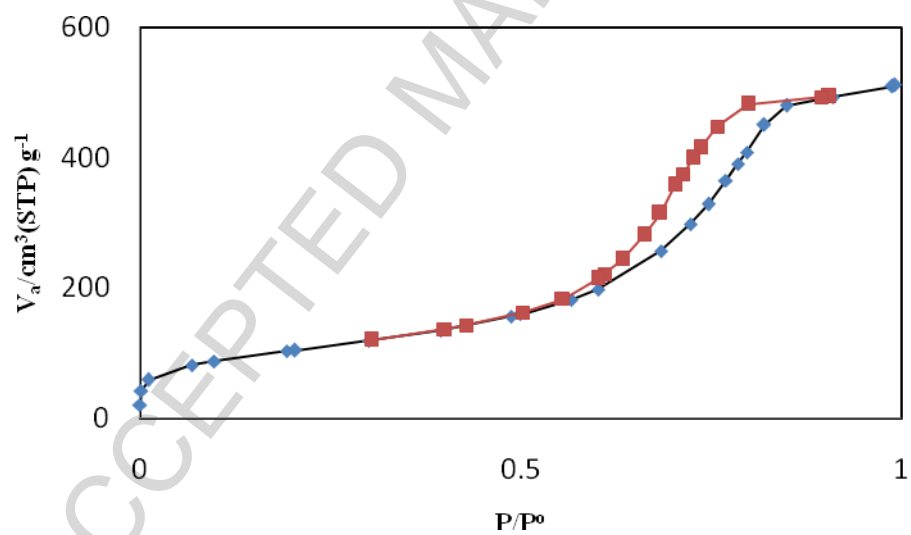


Figure 2. N₂ Adsorption/desorption isotherm of the activated bare silica support.

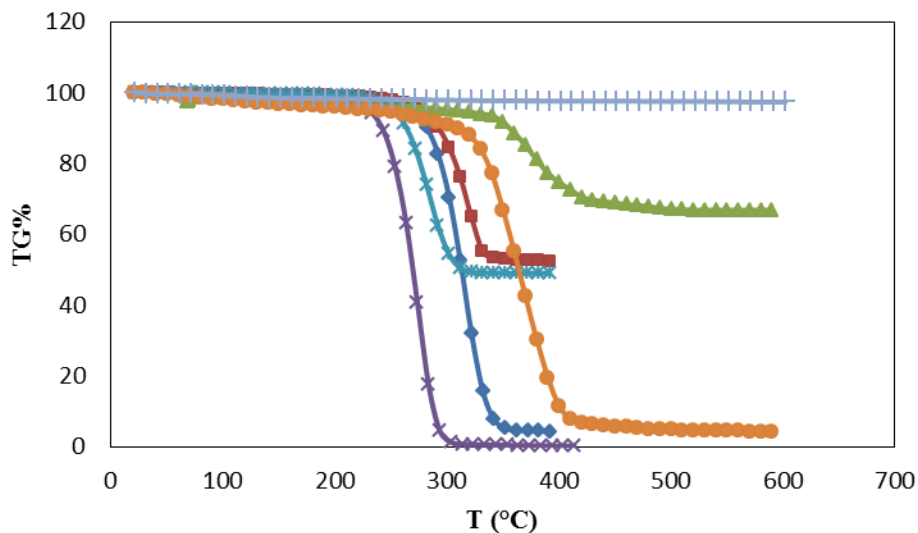


Figure 3. TGA curves of the [bmim][SCN] (×), [bmim][NO₃] (◆), [bmim][HSO₄] (●), [bmim][SCN]-SiO₂ in feed ratio of 1/1(x) [bmim][NO₃]-SiO₂ in feed ratio of 1/1(■), 1/2 (▲), bare SiO₂ (+) (N₂ atmosphere, heating rate of 20 °C/min).

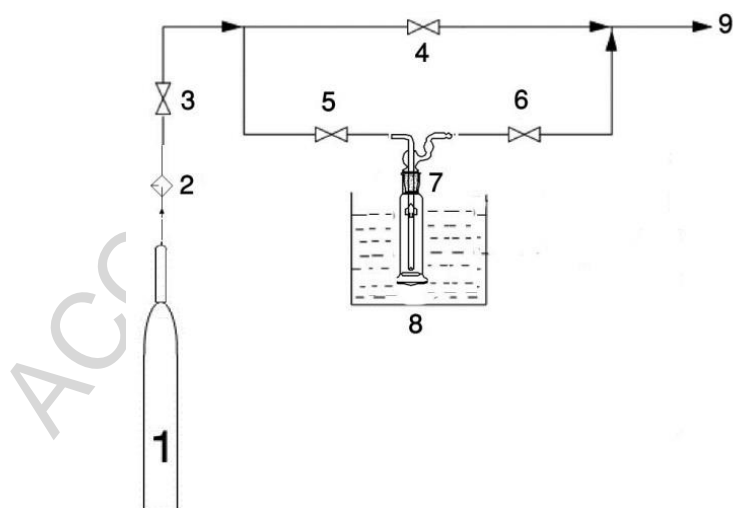


Figure 4. Experimental setup for measuring the adsorbed CO₂ during sorption process (1) CO₂ cylinder; (2) P₂O₅ column; (3-6) Valves; (7) T-shaped glass reactor; (8) water bath; (9) CO₂ outlet for venting.

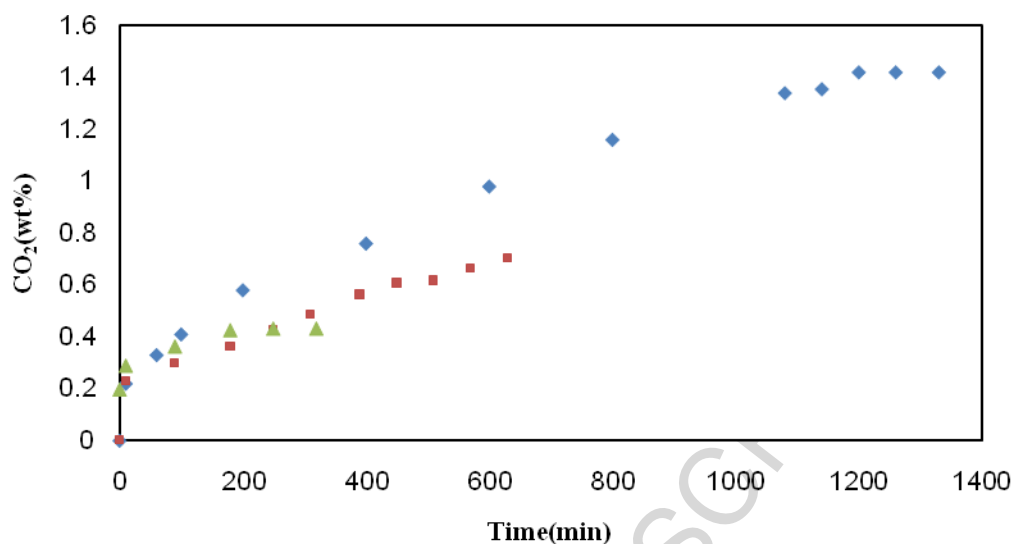


Figure 5. Absorption capacity of [bmim][NO₃] at 25°C(◆), 40°C(■) and 50°C(▲) by passing dry CO₂ with a flow rate of 12 mL/min.

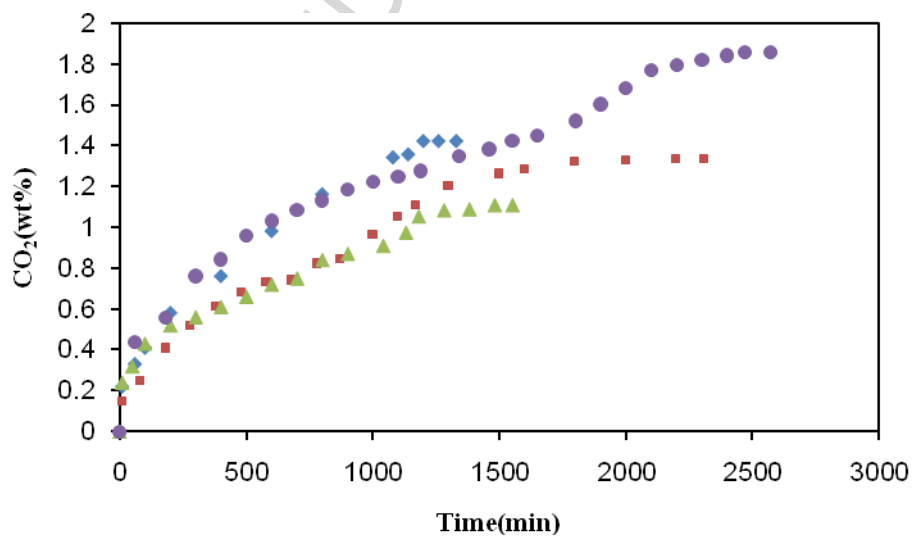


Figure 6. Absorption capacity of [bmim][N(CN)₂] (●), [bmim][NO₃] (◆), [bmim][HSO₄] (■) and [bmim][SCN] (▲) by passing dry CO₂ at 25°C with a flow rate of 12 mL/min.

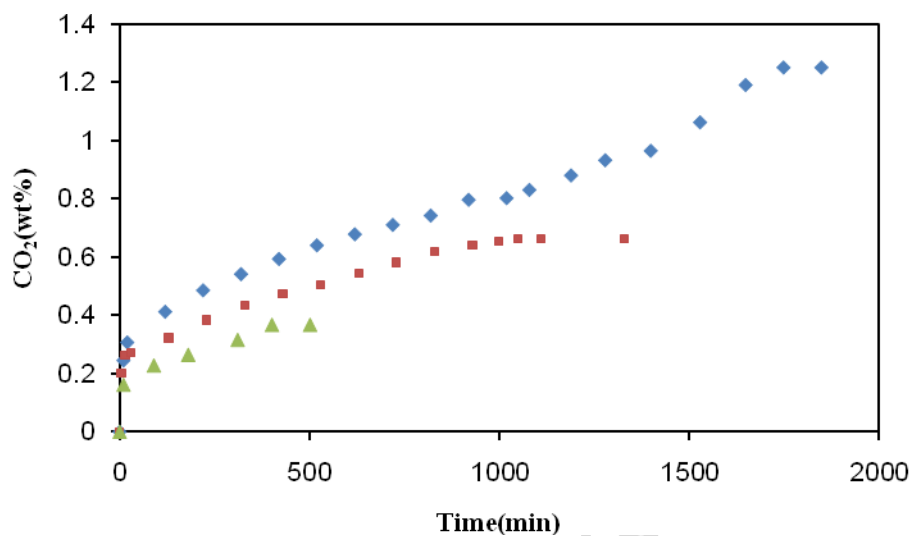


Figure 7. Absorption capacity of [bmim][SCN]-SiO₂ at 25°C(♦),40°C(■) and 50°C(▲) by passing dry CO₂ with a flow rate of 12 mL/min.

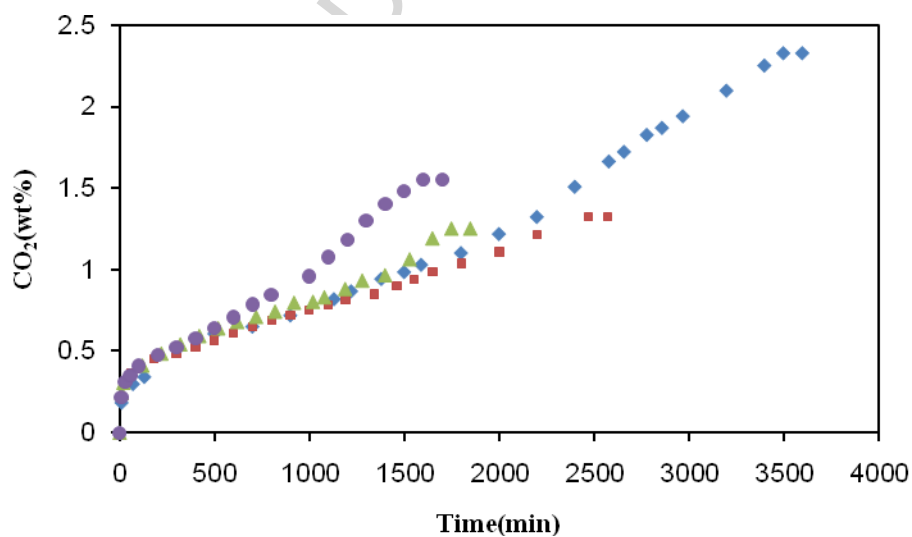


Figure 8. Absorption capacity of [bmim][HSO₄]-SiO₂ (♦), [bmim][NO₃]-SiO₂ (●), [bmim][N(CN)₂]-SiO₂ (■), and [bmim][SCN]-SiO₂ (▲) by transition of dry CO₂ at 25 °C with a flow rate of 12 mL/min.

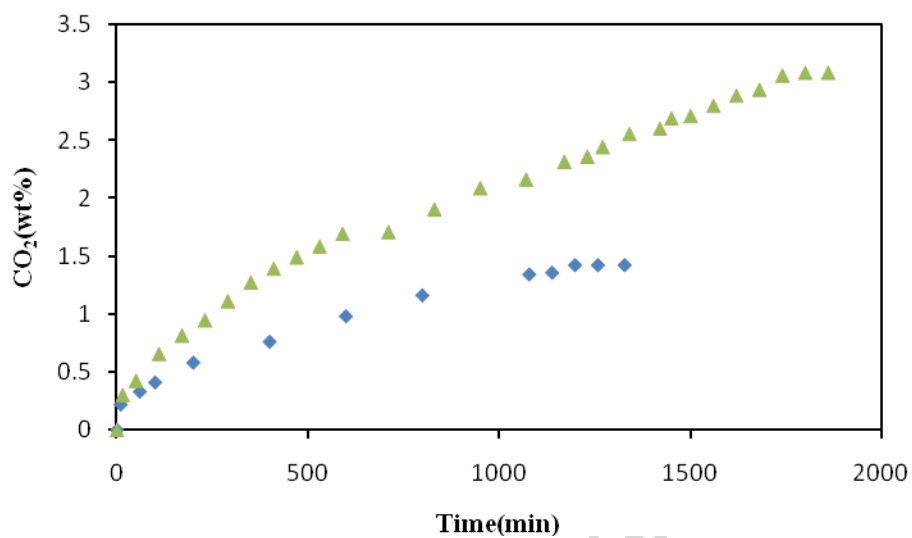


Figure 9. Absorption capacity of the neat [bmim][NO₃] by transition of wet (400 ppm water, ▲) and dry (◆) CO₂ at 25 °C with a flow rate of 12 mL/min.

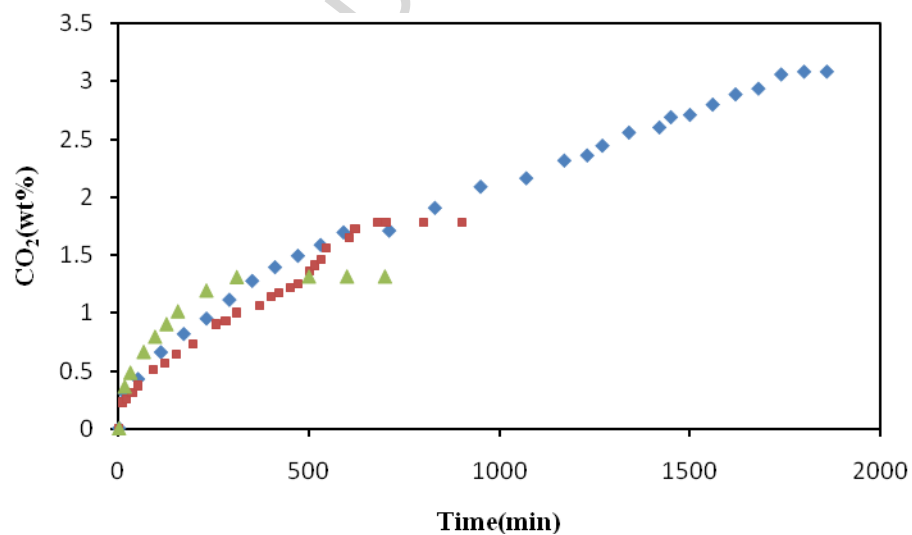


Figure 10. Absorption capacity of [bmim][NO₃] at 25°C(◆),40°C(■) and 50°C(▲) by passing the wet CO₂ (400 ppm water) with a flow rate of 12 mL/min.

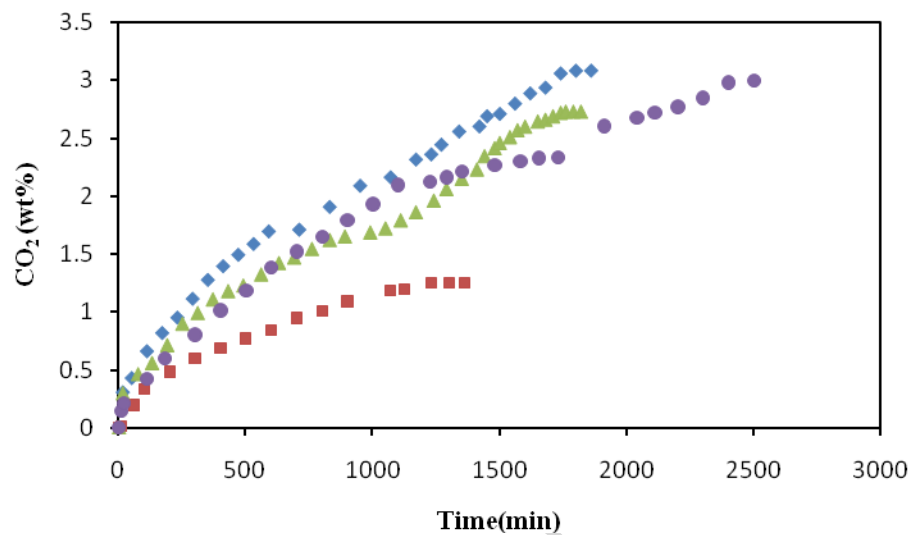


Figure 11. Absorption capacity of [bmim][NO₃] (◆), [bmim][HSO₄] (●), [bmim][N(CN)₂] (▲) and [bmim][SCN] (■) by transition of wet CO₂ (400 ppm water) at 25 °C with a flow rate of 12 mL/min.